Article ID: 1000-324X(2013)12-1376-05 **DOI:** 10.3724/SP.J.1077.2013.13252

Synthesis and Characterization of Nanoporous Graphitic Nanocages by Sulfur-doping Template Method

SHENG Zhao-Min, WANG Ying, CHANG Cheng-Kang, LIU Xiao-Rong, ZHANG Dong-Yun, LIU Yan

(School of Materials Science and Engineering, Shanghai Institute of Technology, Shanghai 201418, China)

Abstract: A new sulfur(S)-doping template approach was demonstrated to fabricate highly nanoporous graphitic nanocages (GNCs) by air-oxidizing the template in the graphitic shells to create nanopores. Sulfur was introduced into graphitic shells, when Fe@C core-shell nanoparticles were prepared and then S-doped GNCs were obtained by removing their ferrous cores. Due to removing S-template, both the specific surface area and the mesopore volume of the GNCs have sharply risen from 540 to 850 m^2/g, 0.44 to 0.90 cm^3/g, respectively. Compared with traditional approaches for highly nanoporous graphitic nanomaterials, present S-template approach can sharply increase specific surface area of GNCs without violently destroying their graphitic structure.

Key words: doping; high specific surface area; graphene; carbon nanohorns; XPS

Recently a wide variety of highly graphitic nanomaterials such as carbon nanotubes (CNTs)[1-3], nanohorns[4-5], closed spherical carbon shells (carbon nanoonions)[6], hollow graphitic nanocages (GNCs)[7-10] and graphenes[11-12] have been prepared with unique chemical or physical properties. However, exploration of the electrochemical applications of those highly graphitic nanomaterials has been hindered, as the large specific surface area is also very important for a catalyst support and supercapacitor electrode materials[1-4,7-10,13]. Unfortunately, the specific surface area of such materials is usually not high (<600 m^2/g)[8-9], because a good graphitization usually trades off property of surface area and surface reactivity[7]. To increase their specific surface area, chemicals such as bases, acids or CO_2 have been introduced to create defects and/or nanopores[14-16], but these methods often violently destroy the graphitic structure. Recently, we have enhanced specific surface area of graphitic nanocages to 535 m^2/g by reducing their shells to a few graphene layers[8]. However, such thin-walled nanocages are always enclosed by the graphitic shells, which greatly constrains molecules diffusion across the shell for full material utilization. To open inner hollow structure, a nitrogen(N)-doped precursor has been heated and then lots of nanopores have formed in the graphitic shell from removing N-doping structure[9]. However, other template approach, such as employing other elements to replace nitrogen for doping, has not been carried out and those novel templates might further increase the surface area of the nanocages.

In this study, we demonstrate a novel sulfur(S)-tem plate approach for increasing the specific surface area of graphitic nanocages and their graphitic structure has been analyzed before and after removing S-template. Sulfur is introduced into graphitic shells, when Fe@C core-shell nanoparticles are prepared and then S-doped GNCs are obtained from removal of their ferrous cores. Porous graphitic structure is prepared by further removing S-doped template.

1 Experimental

Proposed growth process of the highly nanoporous GNCs from S-template approach is shown in Fig. 1. For a typical experiment, the solution was made from 40 mL of iron pentacarbonyl dissolved in 80 mL of carbon disulfide and then the solution supplied by a pump at rate of 60 mL/h was sprayed into a quartz tube furnace set at 800℃ with N_2 as a diluting gas (N_2 flowing rate: 80 L/h). Following thermal pyrolysis of the sprayed solution, Fe@C nanoparticles were formed. To remove the ferrous cores, the Fe@C nanoparticles were stirred in HCl acid at 80℃ for 6 h and then such acid-treated samples were filtered and dried to obtain S-doped graphitic nanocages. For removing S-doping template, the sample was heated in vacuum at 300℃ for 0.5 h or oxidized in air at 350℃ for 0.5 h.

Received date: 2013-05-06; **Modified date:** 2013-06-08; **Published online:** 2013-08-29
Foundation item: Shanghai Municipal Education Commission (J51504, 13YZ118); National Natural Science Foundation of China (21306113, 51074107); Shanghai Institute of Technology (YJ2013-1); Pujiang Talent Project (13PJ1407400)
Biography: SHENG Zhao-Min(1980–), male, PhD. E-mail: zmsheng@sit.edu.cn

Fig. 1　Proposed growth process of the highly porous GNCs prepared from S-template approach

Materials were characterized and analyzed by X-ray diffractometer (XRD) (Bruker AXS), high-resolution transmission electron microscope (HRTEM, JEM-2100F), X-ray photoelectron spectroscope (XPS), Raman spectrum (LabRam-1, Dilor, France; λ=632.8 nm) and nitrogen adsorption/desorption measurement (Quantachrome Instruments).

2　Results and discussion

2.1　Prepared nanoparticles before and after removing ferrous cores

A typical TEM image of the S-doped Fe@C core-shell nanoparticles is shown in Fig. 2(a). Their diameters are ranged from 10–40 nm and the thickness of the shell is 1–3 nm. According to XRD results (Fig. 2(b)), the core of the particles is Fe_3C and FeS. The peaks at around 29.8°, 33.7°, 43.2° and 53.2° can be assigned to the reflections of FeS, which forms from pyrolysis of iron pentacarbonyl and carbon disulfide, and the rest of the peaks are related to the Fe_3C phase. After acid-treatment, the ferrous cores (Fe_3C and FeS) are eliminated, leaving hollow cage structure as shown in Fig. 2(c) and their graphitic shells are enclosed without distinguished nanopores. In the XRD pattern (Fig. 2(d)), the peaks appearing at 26.2°, 44.4° and 78.2° result from diffraction at the (002), (101) and (110) planes of graphite, indicating graphitization of nanocages is high and removal of ferrous cores is complete.

2.2　Graphitic nanocages before and after removing doping structure

XPS is employed to analyzed structure change of sulfur-doping. Before removing the S-doping structure, the acid-treated GNCs shown in Fig. 2(c) have been ana lyzed by XPS to measure content and structure of doping (Fig. 3(a)), which indicates that the sulfur content of the nanocages is 3.3at% and the rest is carbon. The S2p peak (Fig. 3(a)) of sulfur is related to S-doping in graphitic structure rather than FeS cores, and the peaks located between

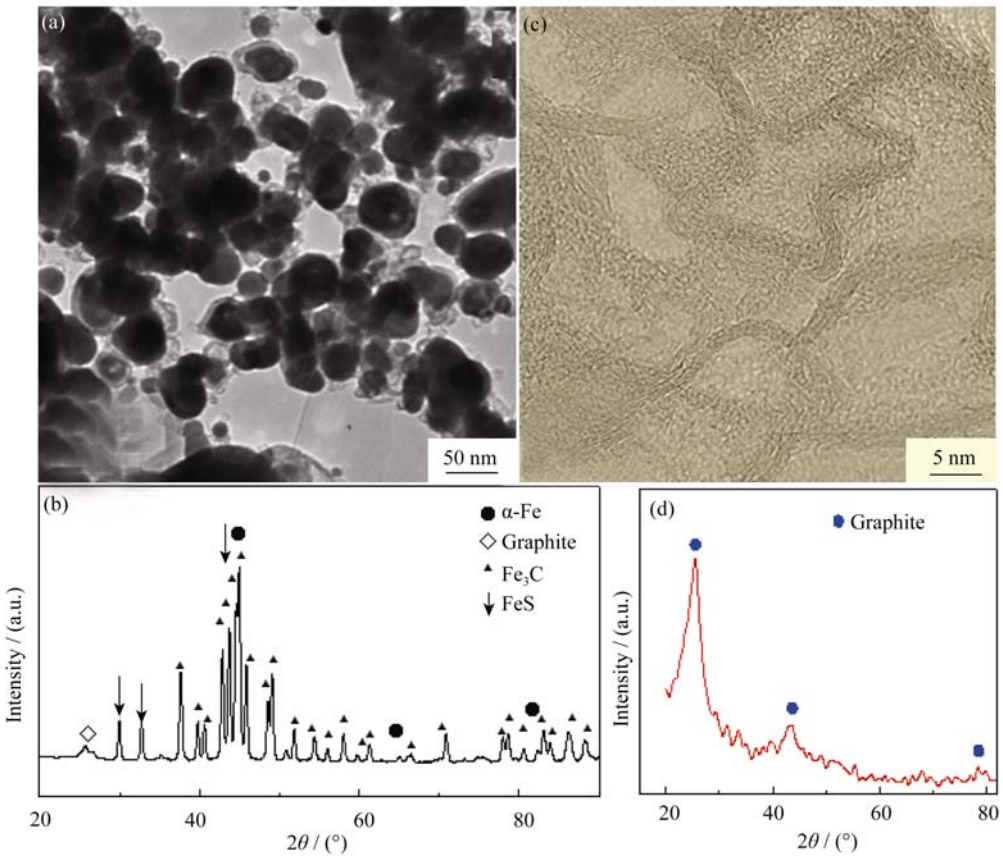

Fig. 2　TEM image (a) and XRD pattern (b) of the S-doped Fe@C core-shell nanoparticles, HRTEM image (c) and XRD pattern (d) of the S-doped GNCs prepared from removing the ferrous cores by acid-treatment

163 and 164 eV might be attributed to S–C bending[17], while the peak located at ~167.1 eV might indicate existence of sulfonate species[17-18], due to acid treating Fe@C nanoparticles might oxidize some S-doping structure. To removal of S-doping structure, air-oxidization is more efficient way than heating in vacuum (Fig. 3(a)), as only sulfonate species might transform into SO_2 but some S–C bending is very stable in the rear condition (Fig. 3(b)). When oxidized in air, all S-doping structure can be oxidized to SO_2, leading to complete removal of S-doping (Fig. 3(a)).

The specific surface area (S_{BET}) and pore volume of graphitic nanocages have been calculated from N_2 adsorption-desorption isotherms (Fig. 4(a)), which shows a higher uptake in the region of low nitrogen pressure (<0.05 P/P_0)

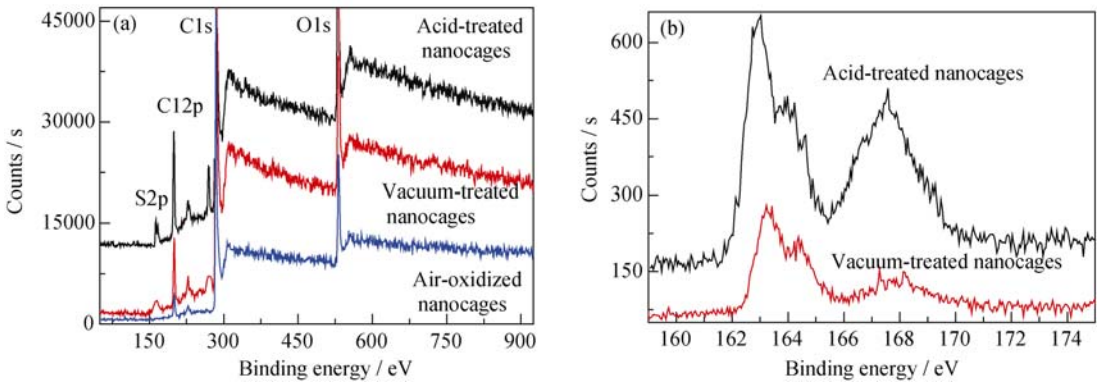

Fig. 3 (a) XPS spectra of S-doped GNCs before (acid- treating) and after (vacuum-heating or air-oxidization) removing doping structure, (b) XPS S2p spectra of GNCs before and after removing doping structure (S-doping structure of air-oxidized GNCs is completely removed and therefore their S2p spectra is not distinguished)

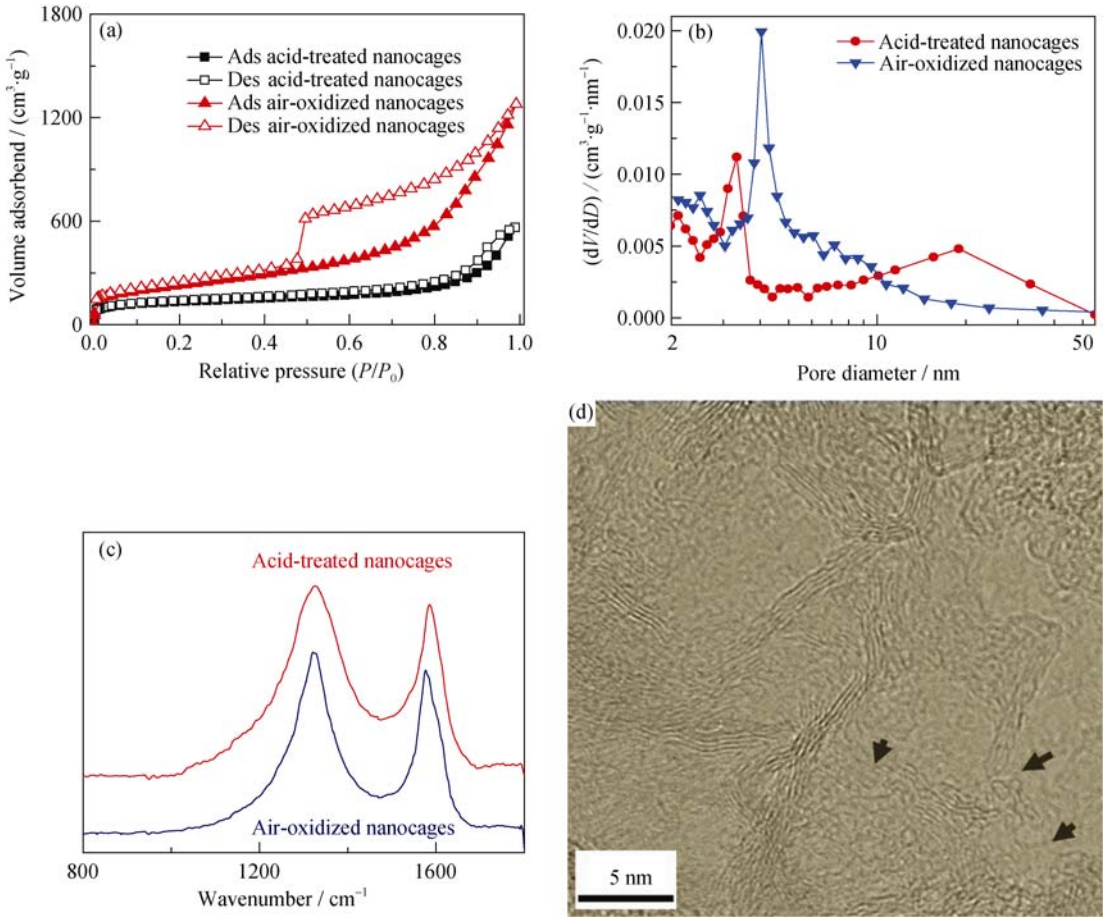

Fig. 4 (a) Nitrogen adsorption/desorption isotherms showing a much higher uptake of N_2 in doping-removed GNCs (air-oxidized GNCs) than S-doped GNCs (Fig. 2(c)). (b) Mesopore size distributions (BJH) showing that there is a much higher population of mesopores in the air-oxidized GNCs than in other ones. (c) Raman spectra of GNCs before and after removing S-doping structure. (d) HRTEM image of the GNCs after removing S-doping structure (nanopores are arrowed)

by the air-oxidized nanocages than that by the nanocages without removal of S-doping structure, indicating the air-oxidized nanocages have more micropores and higher S_{BET}. Furthermore, the air-oxidized nanocages sample has a very pronounced adsorption hysteresis from P/P_0 = 0.4 to ~0.9 (Fig. 4(a)), suggesting that this sample consist of more mesopores than acid-treated nanocages (Fig. 4(b)). This observation suggests that removal of S-doping structure form lots of nanopores in the shells of the nanocages, leading to their specific surface area increases from 540 cm^3/g to 850 cm^3/g and their mesopore volume rises from 0.44 cm^3/g to 0.9 cm^3/g (Fig. 4(a) and (b)).

To investigate the change of graphitic structure, the graphitic nanocages with and without doping structure are analyzed by Raman spectrum (Fig. 4(c)). Both two samples have peaks located near 1324 and 1580 cm^{-1}, Showing good graphitization. However, the peaks of the graphitic nanocages oxidized in air are sharper than those of the ones without air-oxidization. This is attribute to air–oxidizing S-doping structure to remove such structure, which is one kind of defects in the graphitic layers (Fig. 4(c)).

The HRTEM image of the air-oxidized nanocages shows a lot of nanopores exist in their shells arrowed in Fig. 4(d). According to HRTEM image and mesopore size distribution determined by Barrett-Joyner-Halenda (BJH) method (Fig. 4(b)), lots of mesopores (from 0.44 cm^3/g to 0.9 cm^3/g) have formed from removal the S-doping template. However, those mesopores are much bigger than the size of single S atom, which is very likely caused by air-oxidation of S-template: the oxidation of the S atoms heats up C atoms located closely to the S atoms and then those C atoms are burned up in air to create mesopores in the graphitic shells. Compared with previous N-template approach, the present S-template approach performs more effective towards enhancing specific surface area (595 m^2/g *vs* 850 m^2/g) and mesopore volumes (0.72 cm^3/g *vs* 0.9 cm^3/g)[9].

The present GNCs prepared with high specific surface area, mesopore volume and good graphitization can be applied in wide areas as adsorbents, electrode materials, and energy storage media[1,3-14]. With a bigger inner hollow space, the GNCs can be used as gas or radiopharmaceuticals carriers[8]. For instance, as a catalyst support, this material has a better graphitic structure, leading to fast electron-transfer and high stability, and its higher mesopore volume provides better efficient diffusion channels for high utilization of catalysts.

3 Conclusion

In summary, we demonstrate a new S-doping template to fabricate highly nanoporous graphitic nanocages by air-oxidizing S-doped structure in the graphitic shells to violently create nanopores. Due to removing S-template, both the specific surface area and the mesopore volume of the GNCs have sharply risen from 540 m^2/g to 850 m^2/g, 0.44 cm^3/g to 0.9 cm^3/g, respectively. It is discovered that the removal of S atoms during the air-oxidization process creates lots of mesopores in the shells of the GNCs, because the oxidation of the S atoms might burn up C atoms nearby the S. Compared with previous N-template approach, the present S-template approach performs more effective towards enhancing specific surface area (595 m^2/g *vs* 850) and mesopore volumes (0.72 cm^3/g *vs* 0.9)[9]. It should be mentioned that removal of S-doping structure sharply increases specific surface area of GNCs without violently destroying their graphitization. This approach provides a new method to prepare highly nanoporous graphitic materials with potential broad applications in electrochemical energy storage/conversion systems.

References:

[1] Lee Y J, Yi H, Kim W J, *et al*. Fabricating genetically engineered high-power lithium-ion batteries using multiple virus genes. *Science*, 2009, **324(5930):** 1051–1055.

[2] Jiao Z H, Zhang X B, Cheng J P, *et al.* Preparation and characterization of carbon nanotubes/ZnS composite. *J. Inorganic Mater.* 2008, **23(3):** 491–495**.**

[3] Day T M, Unwin P R, Macpherson J V. Factors controlling the electrodeposition of metal nanoparticles on pristine single walled carbon nanotubes. *Nano Lett.*, 2007, **7(1):** 51–57.

[4] Sandanayaka A S D, Ito O, Zhang M F, *et al*. Photo-induced electron transfer in zinc phthalocyanine loaded on single-walled carbon nanohorns in aqueous solution. *Adv. Mater.,* 2009, **21(43):** 4366–4371.

[5] AjimaK, Yudasaka M, Suenaga K, *et al*. Material storage mechanism in porous nanocarbon. *Adv. Mater.*, 2004, **16(5):** 397–401.

[6] Choi M, Altman I S, Kim Y J, *et al*. Formation of shell-shaped carbon nanoparticles above a critical laser power in irradiated acetylene. *Adv. Mater.,* 2004, **16(19):** 1721–1725.

[7] Han S J, Yun Y, Park K W, *et al*. Simple solid-phase synthesis of hollow graphitic nanoparticles and their application to direct methanol fuel cell electrodes. *Adv. Mater.,* 2003, **15(22):** 1922–1925.

[8] Sheng Z M, Wang J N. Thin-walled carbon nanocages: direct growth, characterization and applications. *Adv. Mater.,* 2008, **20(5):** 1071–1075.

[9] Sheng Z M, Guo C X, Li C M. Nitrogen-doping templated

nanoporous graphitic nanocage and its supported catalyst towards efficient methanol oxidation. *Electrochem. Commun.,* 2012, **19(1):** 77–88.

[10] Lu A H, Li W C, Hao G P, *et al*. Easy synthesis of hollow polymer, carbon, and graphitized microspheres**.** *Angew Chem. Int. Ed.,* 2010, **49(9):** 1615–1618.

[11] Wang C, Wang Y L, Zhan L, Synthesis of graphene with microwave irradiation in liquid phase. *J. Inorganic Mater.,* 2012, **27(7):** 769–774.

[12] Guo C X, Yang H B, Sheng Z M, *et al.* Layered graphene/quantum dots for photovoltaic devices. *Angew Chem. Int. Ed.,* 2010, **49(17):** 3014–3017.

[13] Sheng Z M, Wang J N, Ye J C. Synthesis of nanoporous carbon with controlled pore size distribution and examination of its accessibility for electric double layer formation. *Micropor. Mesopor. Mat.,* 2008, **111(2):** 307–313.

[14] Raymundo-Pinero E, Azais P, Cacciaguerra T, *et al.* KOH and NaOH activation mechanisms of multiwalled carbon nanotubes with different structural organization. *Carbon*, 2005, **43(4):** 786–795.

[15] Bekyarova E, Kaneko K, Yudasaka M E, *et al.* Controlled opening of single-wall carbon nanohorns by heat treatment in carbon dioxide. *J. Phys. Chem. B*, 2003, **107(19):** 4479–4484.

[16] Yang C M, Noguchi H, Yudasaka M, *et al.* Highly ultramicroporous single-walled carbon nanohorn assemblies. *Adv. Mater.,* 2005, **17(7):** 866–870.

[17] Gassman G P, Callstrom R M, Martin J C, *et al.* XPS data for linear three-center, four-electron bonding in sulfur species. *J. Am. Chem. Soc.*, 1988, **110(26):** 8724–8725.

[18] Wei X L, Fahlman M, Epstein A J. XPS study of highly sulfonated polyaniline. *Macromolecules*, 1999, **32(9):** 3114–3117.

硫模板法制备多孔石墨纳米笼及其性能表征

盛赵旻, 王 樱, 常程康, 刘晓荣, 章冬云, 刘 艳

(上海应用技术学院 材料科学与工程学院, 上海 201418)

摘 要: 本文研究出一种利用硫模板制备多孔石墨纳米笼的方法, 其核心为利用空气氧化将石墨层中掺杂的硫除去并在原位产生纳米孔洞。硫的掺杂是在碳包裹铁纳米核壳颗粒制备中同时进行的, 随后将其中铁基内核除去即得硫掺杂的石墨纳米笼。将其中的硫除去后, 石墨纳米笼的比表面积(由 540 m^2/g 提高至 850 m^2/g)和介孔孔容(由 0.44 cm^3/g 提高至 0.9 cm^3/g)均有显著提高。与传统制备多孔石墨纳米材料的方法相比, 本方法在显著提高材料比表面积的同时未对纳米笼的石墨化结构有明显破坏。

关 键 词: 掺杂; 高比表面积; 石墨烯; 碳纳米角; XPS

中图分类号: TQ174 **文献标识码:** A